Mix Sustentável

Sustainable hardening of EAF slag mortars by accelerated carbonation: Statistical optimization

Endurecimento sustentável de argamassas com escória FEA por carbonatação acelerada: Otimização estatística

Endurecimiento sostenible de morteros con escoria EAF mediante carbonatación acelerada: Optimización estadística

Heliton Weide[1]
André Lübeck[1]
Alexandre Silva de Vargas[1]
Daniel Assumpção Bertuol[2]
Felipe José da Silva[3]

[1] PPGECAM - Programa de Pós-graduação em Engenharia Civil e Ambiental, Universidade Federal de Santa Maria, Santa Maria, Rio Grande do Sul, Brasil

[2] PPGEQ - Programa de Pós-graduação em Engenharia Química, Universidade Federal de Santa Maria, Santa Maria, Rio Grande do Sul, Brasil

[3] Instituto Federal de Educação, Ciência e Tecnologia do Rio de Janeiro - IFRJ, Rio de Janeiro, Brasil

Correspondence to: helitonweide@gmail.com

ORIGINAL ARTICLE - SCIENTIFIC SECTION
RESPONSIBLE EDITORS: Lisiane Ilha Librelotto, Dr. Eng., Paulo Cesar Machado Ferroli, Dr. Eng.

SUBMITTED ON
03/26/2026
ACCEPTED ON
06/03/2026
PUBLISHED ON
10/15/2026

PID
10.29783/2447-3073.MIX2026.v12.n4.19-51

Standard License Text
This work is licensed under a Creative Commons Attribution 4.0 International License.

Copyright Statement
Authors retain the copyright and grant the journal the right of first publication, with the work simultaneously licensed under a Creative Commons Attribution license, which permits sharing of the work with proper acknowledgment of authorship and initial publication in this journal.

Abstract: Portland cement production generates elevated CO_2 emissions on the order of 500 kg to 600 kg per ton of cement, and this fact drives the development of cements with lower environmental impact. Consequently, metallurgical slag activation methodologies through accelerated carbonation have emerged as a promising alternative to produce clinker-free binders. This study evaluated the effect of process parameters on the compressive strength of mortars produced with electric arc furnace slag (EAFS) and sand in a mix ratio of 1:3. Cylindrical specimens were subjected to accelerated carbonation at a range of temperatures (40 °C, 60 °C and 80 °C), CO_2 pressures (5 bar, 10 bar, 40 bar and 60 bar) and process times (2 h, 4 h and 6 h) and compared to control samples which were not subjected to CO_2 activation. Statistical analysis (ANOVA and Tukey's test) determined that carbonation time was a significant factor for all temperature ranges, while CO_2 pressure was only relevant at 60 °C. Optimized conditions yielded a compressive strength of 12.56 MPa compared to 0.97 MPa of the control sample, an increase of 1,195%. Results confirmed that accelerated carbonation was an efficient methodology to produce sustainable EAFS-based cementitious materials with superior mechanical properties.
Keywords: Accelerated carbonation; Electric arc furnace steel slag; Carbon sequestration.

Resumo: A produção de cimento Portland gera elevadas emissões de CO_2, na ordem de 500 a 600 kg por tonelada de cimento, o que impulsiona o desenvolvimento de ligantes com menor impacto ambiental. Nesse contexto, metodologias de ativação de escórias por carbonatação acelerada têm emergido como uma alternativa promissora para a produção de ligantes isentos de clínquer. Este estudo avaliou o efeito dos parâmetros de processo na resistência à compressão de argamassas produzidas com escória de forno elétrico a arco (EAFS) e areia, em uma proporção de 1:3. Corpos de prova cilíndricos foram submetidos à carbonatação acelerada sob diferentes condições de temperatura (40 °C, 60 °C e 80 °C), pressão de CO_2 (5, 10, 40 e 60 bar) e tempo de processo (2 h, 4 h e 6 h), sendo comparados a amostras de controle não submetidas à ativação por CO_2. A análise estatística (ANOVA e teste de Tukey) indicou que o tempo de carbonatação foi um fator significativo em todas as faixas de temperatura, enquanto a pressão de CO_2 foi relevante apenas a 60 °C. As condições otimizadas resultaram em uma resistência à compressão de 12,56 MPa, em comparação com 0,97 MPa da amostra de controle — um aumento de 1.195%. Os resultados confirmaram que a carbonatação acelerada é uma metodologia eficiente para a produção de materiais cimentícios sustentáveis à base de EAFS, com

Conflict declaration
Nothing to declare.

Funding source
This research was supported by CNPq/MCTI Universal Call 2023, FAPERGS Call 09/2023 - Gaúcho Researcher Program, and FAPERGS Call 10/2024 - ARD/ARC.

propriedades mecânicas superiores.
Palavras-chave: Carbonatação acelerada; Escória de aciaria de forno elétrico a arco; Sequestro de carbono.

Resumen: La producción de cemento Portland genera elevadas emisiones de CO_2, del orden de 500 a 600 kg por tonelada de cemento, lo que impulsa el desarrollo de ligantes con menor impacto ambiental. En este contexto, las metodologías de activación de escorias mediante carbonatación acelerada han surgido como una alternativa prometedora para la producción de ligantes libres de clínker. Este estudio evaluó el efecto de los parámetros de proceso sobre la resistencia a la compresión de morteros producidos con escoria de horno de arco eléctrico (EAFS) y arena, en una proporción de 1:3. Se sometieron probetas cilíndricas a carbonatación acelerada bajo diferentes condiciones de temperatura (40 °C, 60 °C y 80 °C), presión de CO_2 (5, 10, 40 y 60 bar) y tiempo de proceso (2 h, 4 h y 6 h), comparándose con muestras de control no sometidas a activación con CO_2. El análisis estadístico (ANOVA y prueba de Tukey) indicó que el tiempo de carbonatación fue un factor significativo en todos los rangos de temperatura, mientras que la presión de CO_2 fue relevante únicamente a 60 °C. Las condiciones optimizadas dieron como resultado una resistencia a la compresión de 12,56 MPa, en comparación con 0,97 MPa de la muestra de control, lo que representa un aumento del 1.195%. Los resultados confirmaron que la carbonatación acelerada es una metodología eficiente para la producción de materiales cementicios sostenibles a base de EAFS, con propiedades mecánicas superiores.
Palabras clave: Carbonatación acelerada; Escoria de horno de arco eléctrico; Secuestro de carbono.

Como citar: WEIDE, Heliton; LÜBECK, André; VARGAS, Alexandre Silva de; BERTUOL, Daniel Assumpção; SILVA, Felipe José da. Endurecimento sustentável de argamassas com escória FEA por carbonatação acelerada: Otimização estatística. **Sustainable hardening of EAF slag mortars by accelerated carbonation: Statistical optimization**. Florianópolis, v. 12, n. 4, p. 19-51, 2026. DOI: 10.29783/2447-3073.MIX2026.v12.n4.19-51.

1 INTRODUCTION

The cement industry accounts for approximately 8% of total anthropogenic carbon dioxide (CO_2) emissions corresponding to around 2.4 Gt yearly (ANDREW, 2019). In 2019, global production of cement amounted to 4.1 Gt with a corresponding 2.4 Gt of CO_2 emissions or approximately 500 kg to 600 kg of emissions per ton of cement produced (GUO *et al*., 2024). The scale of CO_2 emissions in cement production matches its status as the most consumed material by humans after water, and its emissions make the decarbonization of binders a critical issue for global sustainability (UNEP, 2022).

The International Energy Agency deemed essential the implementation of new technologies to produce carbon-neutral concrete by 2050, aiming to reduce the high greenhouse gases emissions associated with cement production (IEA, 2021). To this end, accelerated carbonation has emerged as an innovative technique which involves using CO_2 absorption to activate cementitious materials. This process promotes the formation of stable carbonate minerals, improving the mechanical performance and chemical stability of the matrix, as reported by Cristino (2024), while simultaneously enabling CO_2 sequestration and contributing to the mitigation of greenhouse gas emissions (YI *et al*., 2021).

On the other hand, the metallurgy sector accounts for approximately 7 % of global CO_2 emissions. This corresponds to approximately 3.7 Gt yearly and an average emission of 2 tons of CO_2 per ton of steel produced (DIGIOVANNI and ECHTERHOF, 2024). Among the various byproducts generated by this industrial activity, slag represents a significant environmental problem due to its chemical composition, with high CaO (24 % to 65 %) and MgO (3 % to 20 %) contents, and consequent high reactivity to CO_2 (BIAVA *et al*., 2024). Consequently, metallurgical slag is proposed to be ideal for producing alternative binders to Portland cement and also mitigating CO_2 emissions (SRIVASTAVA *et al*., 2021). Recent studies have determined that slag has a potential to sequester 370 kg to 420 kg of CO_2 per ton, which would be equivalent to 5% to 8% of the current total emissions from the metallurgical sector (RENFORTH *et al*., 2024).

The technical feasibility of safely and efficiently reusing electric arc furnace slag from steelmaking for the construction industry is an ongoing field of study. This type of slag is generated when scrap metal is used in steel production, and consequently, its chemical composition varies according to the scrap's origin (YILDIRIM; PREZZI, 2011). However, its calcium and magnesium oxide content makes this material suitable for accelerated carbonation, with the additional advantage of substantially increased compressive strength and improved microstructure, which affects durability and density (LI *et al*., 2022).

Electric arc furnace (EAF) steel slag is available in sufficient quantities to justify its large-scale utilization in Brazil. According to the literature, the Brazilian steel industry generates between 19.5 and 20.1

million tons of solid residues annually, of which approximately 25-27% correspond to steelmaking slags (DEUS *et al*., 2020; CARVALHO *et al*., 2024; ANDRADE *et al*., 2021). Furthermore, the total production of steel slags in the country is estimated at approximately 6.25 million tons per year (COSME and FERNANDES, 2025). Considering that the electric arc furnace route accounts for approximately 25% of Brazilian steel production (MANERA *et al*., 2024; HEBEDA *et al*., 2023), the annual generation of EAF slag is estimated to range between 0.9 and 1.1 million tons, corresponding to approximately 75,000-92,000 tons per month.

Regarding storage, the literature does not provide specific quantitative data on accumulated EAF slag stockpiles. Nevertheless, according to Xavier *et al*. (2022) and Guimarães *et al*. (2021), a significant portion of these residues remains deposited in open-air stockyards due to limited reuse opportunities. As a result, extensive areas within steelmaking facilities are occupied by slag deposits, which may remain stored for prolonged periods during natural cooling and aging processes.

Several critical factors affect the strength of slags in a carbonation process with temperature being one of the most relevant. However, in order to improve material properties, the temperature must be adjusted to promote CO_2 permeability while also accounting for humidity in the sample and process pressure. Ko *et al*. (2015) evaluated the carbonation of basic oxygen furnace slag and noted that higher temperatures accelerated the reaction but decreased CO_2 solubility in water, which caused a negative impact on carbonation rates at elevated temperatures. Yi *et al*. (2021) evaluated carbonation of ladle furnace slag and determined that higher temperatures promoted the reaction but also increased instability of the HCO3- ion which decreased its concentration and process efficiency. In the case of steelmaking slag, Srivastava *et al*. (2021) suggested a temperature range between 50 °C and 80 °C to optimize carbonation and hardening of the material.

In addition to temperature, CO_2 pressure also significantly affects compound solubility and increases strength. Yi *et al*. (2021) observed that CO_2 pressure improved carbonation, but it should be closely monitored, as increased pressure also increased calcite solubility and affected final material properties. Regarding time, Srivastava *et al*. (2021) reported that the duration of the carbonation process also significantly impacted slag properties. Varied carbonation process durations were evaluated, from 2 h up to 24 h, and the highest strength gains were observed between 2 h to 4 h from the start.

Ghouleh *et al*. (2015), Zhong *et al*. (2021) and Mo *et al*. (2019) evaluated accelerated carbonation of other types of slag such as basic oxygen slag and magnesium slag for application in mortars. This study proposed an innovative study of activating electric arc furnace slag (EAFS) through accelerated carbonation in order to produce a sustainable mortar. Several parameters were evaluated such as temperature, pressure and duration of exposition time to CO_2 in order to determine their effect on the mechanical properties of the material. A statistical analysis was essential to understand the effects of these factors on developing compressive strength. As such, analysis of variance (ANOVA) and post hoc Tukey's test were used to identify

the ideal process conditions that would maximize mechanical performance of the samples.

The recycling of steel slag within the steelmaking process itself, through grinding, agglomeration, and reintroduction into blast furnaces or electric arc furnaces, is not a practice limited to Brazil but rather a strategy widely adopted in several countries, particularly in regions facing increasing pressure to promote circular economy principles, reduce waste generation, and mitigate the scarcity of mineral raw materials. International studies have reported the development of composites containing steel slags intended for reintegration into metallurgical processes, demonstrating that the valorization of this by-product has become a global trend (LI *et al*., 2021; XU *et al*., 2025). In parallel, the accelerated carbonation of steel slags has emerged worldwide as one of the most promising pathways for CO_2 capture and mineralization associated with the production of sustainable cementitious materials. Recent studies by Pan *et al*. (2024), Yu *et al*. (2024), and Zhang *et al*. (2025) describe accelerated carbonation as a promising technology that has been extensively investigated and is experiencing rapid industrial expansion, with applications in the production of aggregates, blocks, supplementary cementitious materials, and high-performance concretes. Furthermore, recent investigations have reported simultaneous improvements in mechanical strength, volumetric stability, and reduced metal leaching following slag carbonation, further increasing international interest in this technology (BUSTAMANTE *et al*., 2025; ZHANG *et al*., 2026). The literature also indicates that several carbonation routes, including gaseous, aqueous, semi-dry, and supercritical processes, have already reached technological maturity levels approaching industrial implementation in some countries, driven primarily by global decarbonization targets within the construction and steel industries (WANG *et al*., 2024).

This study contributes to the development of sustainable alternatives for the construction sector and, at the same time, offering a contribution to a circular economy through the reuse of industrial waste. Furthermore, accelerated carbonation is an efficient technique for sequestering CO_2 and achieving global greenhouse gas emission reduction targets (IPCC, 2023). The results of this study can provide valuable information for the development of more environmentally friendly and high-performance cementitious materials, promoting the transition to a more sustainable construction sector.

2 MATERIALS

2.1 Electric arc furnace slag (EAFS) from steel production

The electric arc furnace (EAF) steel slag used in this study was collected from a steelmaking plant located in southern Brazil after approximately 10 days of storage in a stabilization yard. The material was obtained in granular form directly from the stockpile rather than as fine powder collected from exhaust or dust collection

systems. Subsequently, the slag was subjected to crushing, drying, homogenization, and grinding until a particle size below 180 µm was achieved. The collection point directly affects the particle size distribution and the concentration of heavy particles in the residue. Materials collected from dust control systems generally exhibit finer particle sizes and higher concentrations of heavy metal-bearing particles, whereas slags collected from stockpiles tend to be more heterogeneous and naturally stabilized. Therefore, grinding was required in this study because the slag was obtained in granular form directly from the industrial stockyard.

After collection, the slag aggregate was oven-dried at 105 °C until mass equilibrium was reached and then quartered and homogenized. The slag was then ground in a ball mill for 6 h until reached a particle size of less than 180 µm. The chemical composition of the EAFS is presented in Table 1.

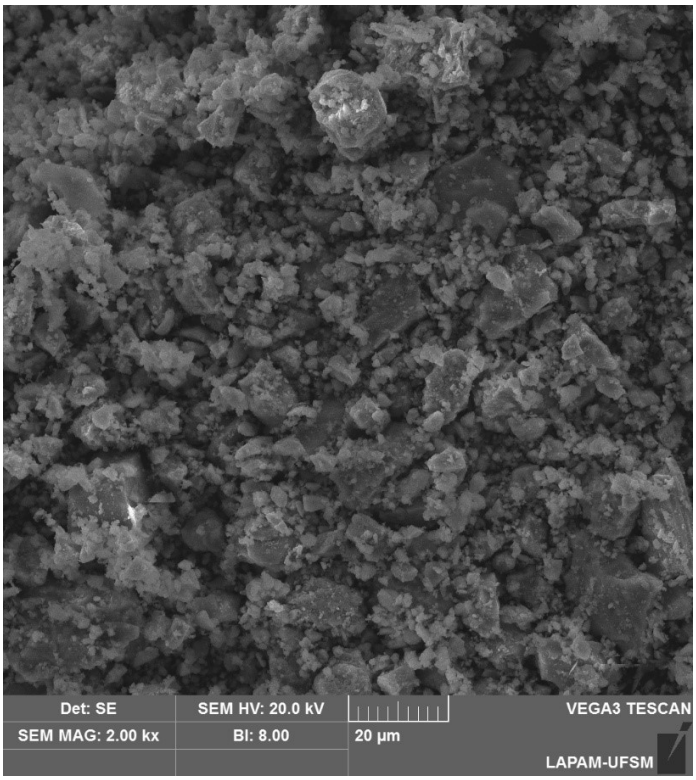
Table 1 - Chemical composition of EAFS in oxide form, as determined from X-ray fluorescence (XRF).

Compound	(% by mass)
CaO	28.36
Fe_2O_3	28.23
SiO_2	18.43
MgO	15.37
MnO	6.27
Al_2O_3	2.71
TiO_2	1.00
P_2O_5	0.18
Loss on ignition	0.38

Source: elaborated by the authors.

The chemical composition of the EAF slag was characterized by the predominance of calcium oxide (CaO) and iron oxide (Fe_2O_3), in agreement with the results reported by Martins *et al*. (2021). The specific surface area determined by the BET method was 1.3147 m²/g. The morphological characterization of the particles was performed using scanning electron microscopy (SEM) at the Laboratory of Construction Materials (LAPAM/UFSM). Figure 1 presents the SEM micrograph of the EAF slag obtained at a magnification of 2000x, allowing the observation of the surface morphology and particle distribution after the grinding process.

Figure 1: Morphology of EAF slag particles observed by scanning electron microscopy (SEM) at a magnification of 2000x.



Source: elaborated by the authors.

As shown in Figure 1, the EAF slag particles exhibit a heterogeneous morphology, with a wide variation in size and predominantly irregular shapes. Particles with angular contours are also observed, together with a smaller proportion of more rounded particles, characteristics commonly reported in the literature for electric arc furnace steel slags. In addition, the particles present a rough surface marked by irregularities and superficial pores, resulting in a coarse texture. These observations are consistent with the findings reported by Sukmak *et al*. (2023) and Akbari *et al*. (2024), who associated this morphology with the cooling, crushing, and grinding processes applied after slag generation.

2.2 Sand

The sand used in mortar production was quartz sand, supplied by the Instituto de Pesquisas Tecnológicas de São Paulo (IPT). It was compliant to the requirements of standard NBR 7215 (ABNT, 2019) and classified in four particle size fractions (1.2 mm, 0.6 mm, 0.30 mm and 0.15 mm). These fractions were used in equal proportions in order to ensure homogeneity and workability of all mixtures.

2.3 Water

The water used in the mixtures was municipal water from the city of Santa Maria, RS, Brazil.

2.4 Carbon dioxide (CO_2)

Carbon dioxide (CO_2) used in accelerated carbonation was liquefied at high pressure (57.3 bar at 20°C) and classified as 99.99 % pure.

3 METHODOLOGY

3.1 Molding of samples

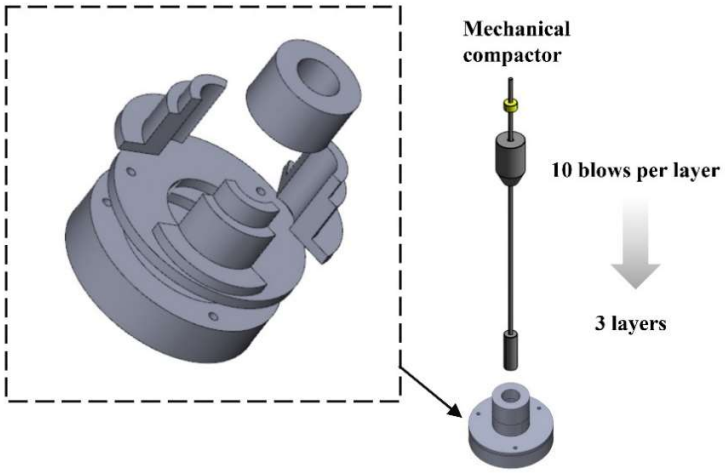
Mortars samples produced from EAFS were molded in cylindrical shapes without end caps or surfacing for compressive strength tests. The mortar consisted of a mix ratio of 1:3 of EAFS and sand. The 1:3 binder-to-sand ratio was adopted because it represents a proportion widely established in technical standards and experimental studies on mortars, being commonly considered a reference mixture for the evaluation of mechanical, microstructural, and durability properties. NBR 7215 (2019), which served as the methodological basis for this study, specifies the procedures for determining the compressive strength of cylindrical mortar specimens and adopts a 1:3 mass ratio for mixture preparation. However, the standard was originally developed for Portland cement-based mortars, whereas in the present study the mixture was adapted by replacing Portland cement with EAF slag as the binding material. An increase in the sand content generally leads to reductions in workability and compressive strength due to the greater friction between particles and the lower amount of binding paste available to coat the aggregates, potentially resulting in significant losses in mechanical performance (CAO *et al*., 2022; HWALLA *et al*., 2023). Conversely, reducing the sand content increases the binder paste fraction, which may enhance strength development, although it can also increase water demand and adversely affect the rheological stability of the mixture (DENG and ZHENG, 2023).

As noted previously, the sand was a mixture of equal proportions of four particle size fractions. Dry material moisture content was maintained at 7 % to ensure workability and integrity during molding. Molding was conducted on a custom three-part mold to produce samples 2 cm in diameter and 3.5 cm in height, to be compatible with the dimensions of the CO_2 accelerated activation reactor.

Mortar was mixed manually, as the small amount of material required to produce a batch of 6 cylindrical samples (160.45 g) made it unsuitable for mixing in a mechanical mixer. Sand and EAFS were mixed manually

for 60 s. Water was added and the mixture homogenized for 90 s. Samples were then manufactured by loading the mortar in the three-part mold in 3 layers settled with a mechanical compactor each time. The mechanical compactor consisted of a 0.5 kg free-falling metallic tamper attached to a metallic rod 45 cm in length. In order to ensure a homogeneous compaction, each layer was tamped 10 times. Figure 2 shows an illustration of the three-part mold and mechanical compactor.

Figure 2 - Compaction process.



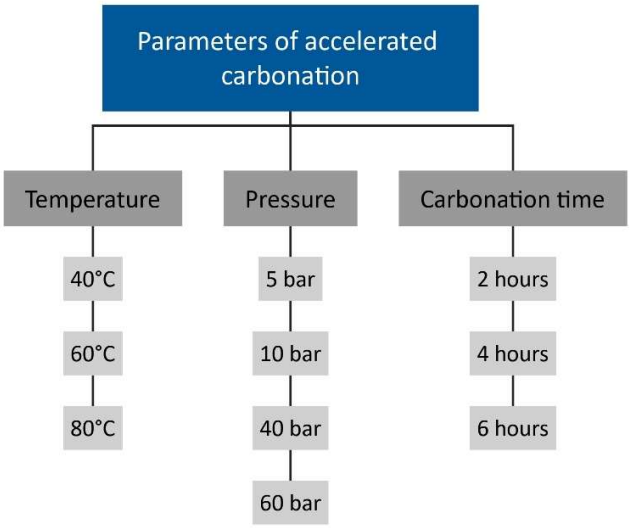
Source: elaborated by the authors.

After preparation, samples were subjected to two distinct processes: accelerated carbonation in a pressurized CO_2 chamber or natural carbonation in a climate-controlled room. Samples that underwent natural carbonation were used as references.

3.2 Accelerated carbonation process

The accelerated carbonation process of EAFS with pressurized CO_2 was organized as a series of tests with controlled parameters. There were: temperatures of 40 °C, 60 °C and 80 °C; CO_2 pressures of 5 bar, 10 bar, 40 bar and 60 bar and duration of process of 2 h, 4 h, and 6 h. Figure 3 presents an overview of the accelerated carbonation parameters evaluated in this study.

Figure 3: Controlled parameters used in EAFS accelerated carbonation tests in a pressurized CO_2 environment.



Source: elaborated by the authors.

Samples were subjected to the accelerated carbonation processes with a combination of the parameters shown in Figure 3 immediately after molding. Compressive strength was evaluated 7 days after the start of the process. Samples were not capped or surface-treated prior to testing.

In studies involving steel slags and activated materials, compressive strength is frequently adopted as the primary response variable because it is directly associated with the load-bearing capacity and structural application potential of the material (SRIVASTAVA et al., 2023). Furthermore, the analyzed study indicates that the main objective of the research was to evaluate the effect of accelerated carbonation on the mechanical development of mortars, particularly as a function of carbonation variables such as time, pressure, and temperature. In this context, compressive strength was selected as the most sensitive parameter for assessing the influence of these processing conditions and quantifying the resulting changes in material performance.

The evaluation of mechanical strength under the simultaneous variation of multiple parameters has become an increasingly relevant research topic because recent studies have demonstrated that the behavior of carbonated cementitious materials cannot be adequately explained through simplified or linear approaches. Unlike traditional methodologies, in which a single factor is varied independently, current research indicates that mechanical performance results from the complex interaction among variables such as CO_2 concentration, carbonation time, pressure, temperature, humidity, precursor chemical composition, and curing conditions. These parameters act synergistically on hydration, carbonation, and microstructural development mechanisms, often producing non-linear responses in which the same material may exhibit an initial increase in strength

followed by a subsequent decline depending on the intensity and duration of the treatment (NGUYEN et al., 2024; ZHOU et al., 2026). Therefore, investigating mechanical strength under multiple processing parameters is not merely a methodological expansion but rather a necessary scientific approach for understanding the highly sensitive and interdependent behavior of cementitious materials containing carbonated slags and industrial residues. Such an approach enables the simultaneous optimization of mechanical performance, microstructural stability, and CO_2 sequestration capacity. The parametric analysis of this study was planned around 3 experimental tables each corresponding to temperatures of 40 °C, 60 °C and 80 °C. Each table contained meshes of combinations of minimum, intermediate and maximum values of all controllable parameters (time, pressure and temperature). These experimental plan meshes allowed the study of the compressive strength of the EAFS mortar along parameters of time, pressure and temperature in 3 levels without the need for a complete factorial analysis. Table 2 presents the experimental plan of each temperature table with meshes marking specific configurations of the accelerated carbonation process as well as the statistical analysis conducted on each mesh.

Table 2: Experimental plan meshes applied to evaluated compressive strength of EAFS mortars with accelerated carbonation.

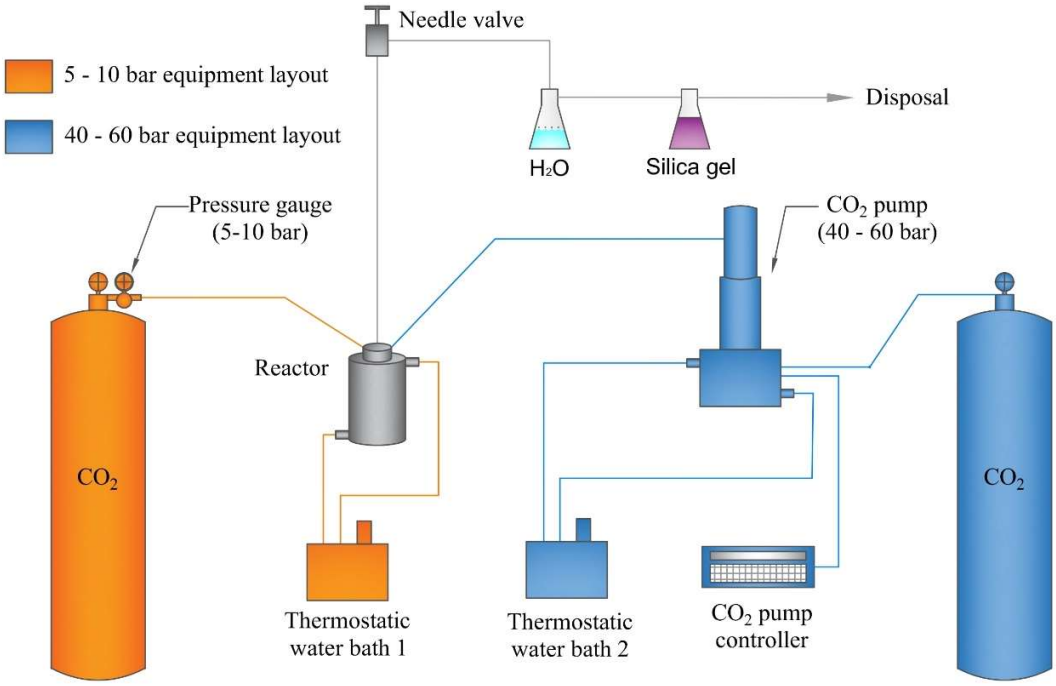
Temperature = 40 °C					Statistical analysis tool
Time (h)	Pressure (bar)				Spearman's correlation matrix
	05	10	40	60	
2		X	X		
4	X			X	
6		X	X		
Temperature = 60 °C					Spearman's correlation matrix
Time (h)	Pressure (bar)				
	05	10	40	60	
2		X	X		
4	X			X	
6		X	X		
Temperature = 80 °C					Spearman's correlation matrix
Time (h)	Pressure (bar)				
	05	10	40	60	
2		X	X		
4	X			X	
6		X	X		

Source: elaborated by the authors.

3.3 Accelerated carbonation apparatus

The apparatus used in the accelerated carbonation process had 2 distinct configurations based on the CO_2 pressure. System 1 handled pressures of 5 bar and 10 bar while System 2 handled pressures of 40 bar and 60 bar, the latter requiring a pressure pump. These systems are schematically shown in Figure 4.

Figure 4: Schematic of accelerated carbonation system for EAFS with System 1 (orange, 5 bar and 10 bar) and System 2 (blue, 40 bar and 60 bar).

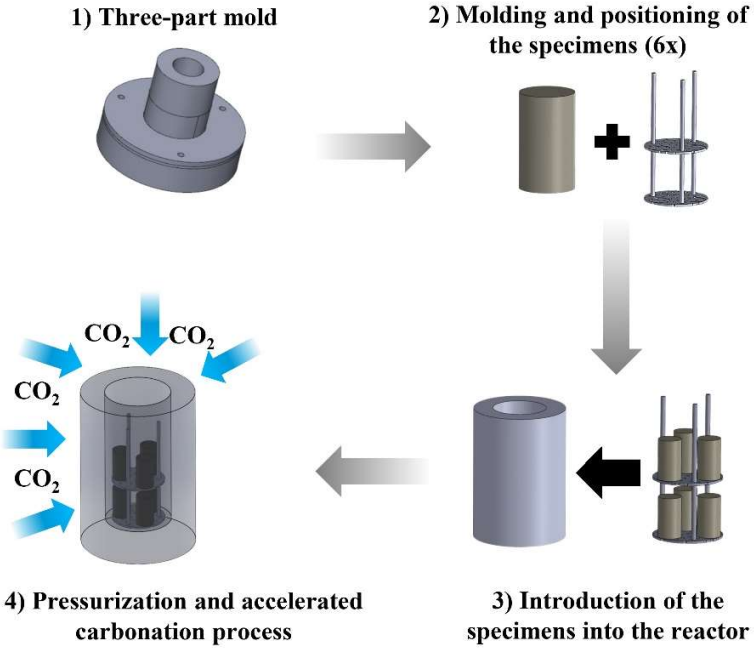


Source: elaborated by the authors.

3.4 Accelerated carbonation process methodology

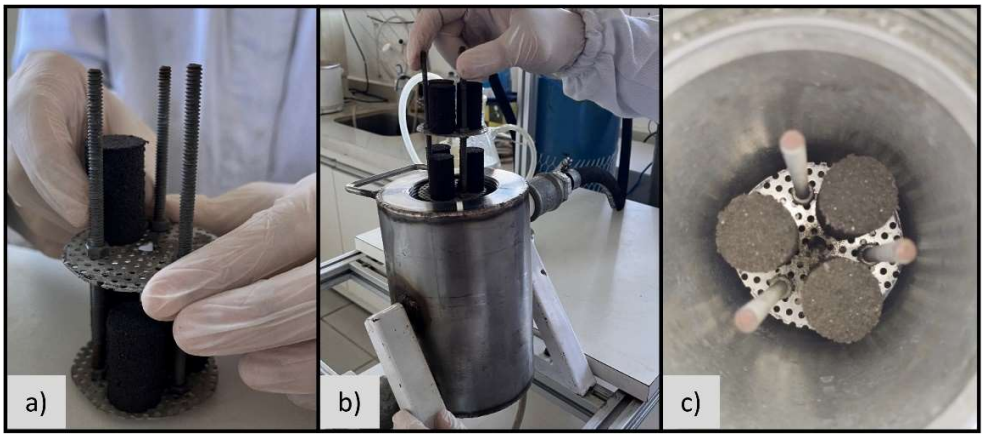
The accelerated carbonation process used in this study was the gas-solid or dry mode with no relative humidity control inside a reactor. Each batch contained 6 cylindrical samples placed inside the reactor on a perforated plate to ensure CO_2 flow. After placement, the reactor was sealed and samples were exposed to the selected combination of temperature, pressure and time. Figure 5 presents a schematic procedure of the molding and the accelerated carbonation processes while Figure 6 shows the experimental procedures of mounting samples in the reactor.

Figure 5: Schematic procedure for accelerated carbonation of EFAS samples.



Source: Adapted from Weide (2024).

Figure 6: Placement of samples inside reactor: a) placement of samples of perforated plate; b) samples being placed in the reactor and c) top view of samples in the reactor prior to sealing.



Source: Weide (2024).

Once the pre-determined process time was reached, the reactor was depressurized and samples removed. After removal, samples were stored in a climate-controlled room kept at 20 °C ± 2 °C for 7 days until compressive strength tests.

3.5 Compressive strength analysis

Axial compressive strength tests were conducted at the Civil Construction Materials Laboratory (Laboratório de Materiais de Construção Civil - LMCC) at UFSM. The apparatus used was an Instron 500HDX-64-67B press with a load rate of 0.05 mm/s. Control samples not subjected to accelerated carbonation were tested at 7 days, 28 days and 91 days of age until rupturing while samples subjected to accelerated carbonation were tested at 7 days of age. Testing was conducted on 6 samples of each configuration.

3.6 Statistical Analysis

Compressive strength test results were analyzed with respect to dispersal to detect outliers with the standard deviation as the chosen parameter. Individual strength values that were measured to exceed plus or minus one standard deviation were considered anomalous and discarded. The average value was then calculated with the remaining samples of the test.

An analysis of the effects of controlled parameters (temperature, pressure and time) was conducted with an analysis of variance (ANOVA) method complemented with a post hoc Tukey's test with a significance level of 95 %. After discarding outlier results, the analysis started with Spearman's correlation (ρ) in order to determine the effect of controlled parameters on the response variable (compressive strength). Spearman's correlation coefficient indicates the relation between an independent variable (X) and a dependent variable (Y). The coefficient is positive when Y increases with an increase in X and negative if Y increases as X decreases (BAUER, 2007). Additionally, a coefficient of zero indicates no clear trend of Y with respect to X while values close to 1 or -1 indicate strong correlation between variables. Dancey and Reidy (2019) proposed correlation (ρ) intervals between 0.10 and 0.30 for a weak correlation, 0.40 and 0.60 for a moderate correlation and 0.70 to 1.0 for a strong correlation.

An ANOVA analysis indicates if significant differences exist between groups but does not identify which groups are different. Consequently, complementary tests such as Tukey's test are used to compare two averages and identify which contains significant differences (PCZIECZEK *et al*., 2019). A p-value below 0.05 indicates a significant effect of the variable and was used in this study with a confidence level of 95 %. These analyses were conducted with JAMOVI v.2.3.21 software (JAMOVI, 2024).

3.7 Scanning Electron Microscopy (SEM) Analysis

The morphological characterization of the samples was performed by scanning electron microscopy (SEM) at the Laboratório de Microscopia of the Federal University of Santa Maria (UFSM), using a JEOL JSM-6360 scanning electron microscope. Micrographs were obtained at different magnifications to evaluate

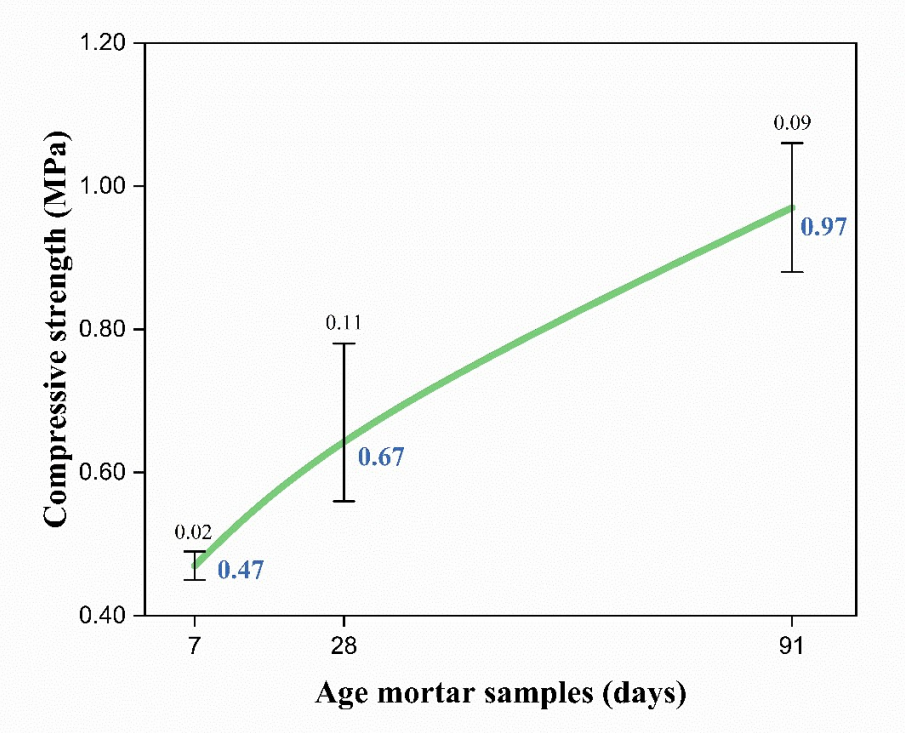
particle morphology and the microstructural changes promoted by the accelerated carbonation process. The microscope is equipped with a QUEST energy-dispersive X-ray spectroscopy (EDS) system manufactured by ThermoSystem.

4 RESULTS

4.1 Compressive strength of control group EAFS mortars (without activation)

Figure 7 presents average axial compressive strength tests results of EAFS mortars not subjected to accelerated carbonation under pressurized CO_2. Tests were conducted on the samples at 7 days, 28 days and 91 days of age. Also presented are error bars representing the standard deviation of each average.

Figure 7: Average axial compressive strength at 7 days, 28 days and 91 days of EAFS mortars not subjected to accelerated carbonation.



Source: elaborated by the authors.

Figure 7 showed a gradual increase in compressive strength up to 91 days and was in accordance with the work of Sun *et al*. (2022). However, Sun *et al*. (2022) also underscored that steel slag had low reactivity and consequently the gains in strength were small over time. Indeed, results of this study showed that at 91 days, the increase in strength of the samples not subjected to accelerated carbonation was in the order of 1

MPa.

4.2 Compressive strength of EAFS mortars subjected to accelerated carbonation from pressurized CO_2

Average axial compressive strength results of EAFS mortars at 7 days of age subjected to accelerated carbonation from pressurized CO_2 are shown in Table 3. The number of samples in the table was less than the total number of samples tested (6 of each combination) due to the exclusion of outlier measurements.

Table 3: Average axial compressive strength of EAFS mortars at 7 days of age subjected to accelerated carbonation.

Temperature (°C)	Time (h)	Pressure (bar)	Samples	Compressive strength (MPa)	SD (MPa)	CV
40	**2**	5	3	**7.49**	0.74	9.8%
		60	3	**9.83**	0.30	3.0%
	4	10	4	**9.85**	0.41	4.1%
		40	3	**10.58**	1.25	11.8%
	6	5	4	**8.43**	0.46	5.4%
		60	3	**9.30**	1.21	13.0%
60	**2**	5	3	**6.91**	0.59	8.6%
		60	5	**6.60**	0.60	9.2%
	4	10	5	**9.88**	0.34	3.5%
		40	3	**7.82**	1.20	15.3%
	6	5	3	**12.16**	0.37	3.0%
		60	3	**8.98**	0.46	5.1%
80	**2**	5	6	**8.22**	0.68	8.3%
		60	3	**7.97**	1.20	15.1%
	4	10	5	**8.49**	0.73	8.6%
		40	4	**8.24**	0.99	12.0%
	6	5	4	**10.42**	0.99	9.5%
		60	3	**9.16**	1.05	11.4%

Source: elaborated by the authors.

Table 3 shows that the highest average compressive strength was 12.16 MPa on EAFS mortars subjected to the combination of 60 °C of temperature, 5 bar of CO_2 pressure and 6 h of process time. In comparison, the lowest average strength was measured at 6.60 MPa for the combination of 60 °C, 60 bar and 2 h.

Comparing the results, the highest average compressive strength of the control group was 0.97 MPa at 91 days of age. In contrast, activated samples under pressurized CO_2 achieved a peak of 12.16 MPa which corresponded to an increase of 1,154 % with respect to the control group. Moreover, this expressive gain in strength was achieved after only 6 h of activation. Similarly, comparing the lowest strength of 6.60 MPa measured in the activated samples to the 0.97 MPa of the control group, the gain in strength was 580 %.

4.3 Effect of controlled factors of accelerated carbonation process (time, pressure and temperature) on compressive strength of EAFS mortar

The effect of controlled factors (time, pressure and temperature) in the activation process of EAFS mortar was evaluated with Spearman's correlation matrix. The general correlation matrix is presented in Table 4 and was evaluated from compressive strength results of the configurations contained in the experimental plan and meshes of Table 2.

Table 4: General Spearman's correlation matrix of controlled factors of compressive strength of accelerated carbonation EAFS mortar.

		Time	Pressure	Temperature
Compressive strength	ρ	0.500	-0.075	-0.16
	p-value	< .001	0.546	0.197

Note: ρ > 0, proportional correlation; ρ < 0, inversely proportional correlation; ρ ≈ 0, weak correlation; p-value > 0.05, non-significant effect; p-value < 0.05, significant effect.
Source: elaborated by the authors.

Results of Table 4 indicated that, based on all experimental arrangement of Table 2, time was the only significant variable in developing compressive strength while pressure and temperature did not have a significant effect. However, different correlation patterns were observed when each temperature (40 °C, 60 °C and 80 °C) was evaluated separately.

4.4 Effect of time of accelerated carbonation process on compressive strength of EAFS mortar.

The effect of time of the accelerated carbonation process was evaluated for the configurations listed in the experimental plan and meshes of Table 2. Statistical analyses of the compressive strength of EAFS mortar for each temperature and configuration are presented in Tables 5, 6 and 7.

Table 5: Spearman's correlation matrix of compressive strength of accelerated carbonation EAFS mortar at 40 °C with respect to variations in time and pressure.

		Time	Pressure
Compressive strength	ρ	-0.061	0.591
	p-value	0.8	0.006

Note: ρ > 0, proportional correlation; ρ < 0, inversely proportional correlation; ρ ≈ 0, weak correlation; p-value > 0.05, non-significant effect; p-value < 0.05, significant effect.
Source: elaborated by the authors.

Table 6: Spearman's correlation matrix of compressive strength of accelerated carbonation EAFS mortar at 60 °C with respect to variations in time and pressure.

		Time	Pressure
Compressive strength	ρ	0.784	-0.336
	p-value	< 0.001	0.030

Note: ρ > 0, proportional correlation; ρ < 0, inversely proportional correlation; ρ ≈ 0, weak correlation; p-value > 0.05, non-significant effect; p-value < 0.05, significant effect.
Source: elaborated by the authors.

Table 7: Spearman's correlation matrix of compressive strength of accelerated carbonation EAFS mortar at 80 °C with respect to variations in time and pressure.

		Time	Pressure
Compressive strength	ρ	0.500	-0.200
	p-value	0.011	0.337

Note: ρ > 0, proportional correlation; ρ < 0, inversely proportional correlation; ρ ≈ 0, weak correlation; p-value > 0.05, non-significant effect; p-value < 0.05, significant effect.
Source: elaborated by the authors.

Results show that effects of time and pressure were different for each temperature. Pressure had a significant effect only at 40 °C, time and pressure were significant at 60 °C and only time was significant at 80 °C. These results indicated that there were optimum levels of each control variable of the process. Additionally, at 40 °C, pressure had a proportional relation to compressive strength but became inversely proportional at 60 °C. Meanwhile time had a directly proportional relation to compressive strength at 60 °C and 80 °C.

At 40 °C, the increase in strength proportional to an increase in pressure could be related to the solubility of CO_2 in the water used in mixing. Loodts *et al*. (2014) stated that a decrease in temperature increased CO_2 dissolution in water mixtures while Wang *et al*. (2023) confirmed that increases in pressure increased CO_2 solubility in water. Thus, it was possible that process conditions were favorable for the dissolution of CO_2 in the water present in the EAFS mortar. This would indicate that CO_2 pressure had a significant effect on

compressive strength as shown in Table 5.

At 80 °C, the only significant factor for the increase in strength was time and this fact could be related to less formation of mineral phases like calcite. Luo *et al*. (2021) determined that calcite formation improved between 30 ℃ and 60 ℃ and decreased at 90 ℃. Christmas and Bassingthwaighte (2017) also noted that CO_2 solubility decreased as temperature increased which would explain the non-significant role of CO_2 pressure in compressive strength development shown in Table 7.

Among the combinations listed in the experimental plan meshes of Table 2, the highest compressive strength (12.16 MPa) was achieved for samples at 60 °C and 6 h of process and was in agreement with Luo *et al*. (2021). This result was also in agreement with Pan *et al*. (2016) and Pan *et al*. (2020), which observed that there was a temperature range limit between 50 °C and 60 °C for accelerated carbonation conversion and its efficiency decreased at higher temperatures.

The configuration mesh of 60 °C was significantly affected by both time and pressure of the process and also yielded the highest compressive strength. Consequently, this temperature was used as the baseline for a subsequent statistical analysis with ANOVA and post-Hoc Tukey's tests. However, since the mesh was incomplete, additional experiments were conducted to complete the data set with all 4 variations of pressure and 3 exposure times. The new mesh with compressive strength results is shown in Table 8.

Table 8: Average compressive strength results (MPa) for new 60 °C mesh.

Time (h)	Compressive strength (MPa)				Statistical analysis tools
	Pressure (bar)				
	5	10	40	60	ANOVA Tukey's test
2	6.91	6.68	6.83	6.60	
4	8.65	9.88	7.82	7.81	
6	12.16	12.56	9.43	8.98	

Source: elaborated by the authors.

4.5 Analysis of Variance (ANOVA) of compressive strength results at 60 °C

An ANOVA was conducted on the results from the combination of factors of Table 8. The factors evaluated were time, pressure and the combined effect of time and pressure on the development of compressive strength. Results are shown in Table 9.

Table 9: ANOVA of compressive strength at 60°C.

	Sum of squares	DF	Mean of sum of squares	F	p
Time	98.8	2	49.41	85.21	< 0.001
Pressure	29.6	3	9.86	17.01	< 0.001
Time × Pressure	21.1	6	3.51	6.07	< 0.001
Residual	17.4	30	0.58		

Obs: carbonation times of 2 h, 4 h and 6 h; pressure values of 5 bar, 10 bar, 40 bar and 60 bar; DF = degrees of freedom; F = F-statistic; p = p-value with p > 0.05 non-significant and p < 0.05 significant

Source: elaborated by the authors.

Results from ANOVA indicated that time, pressure and the interaction between them had significant effects on compressive strength at 60 °C. The effect of time at 60 °C was further evaluated with a Post Hoc Tukey's test and the results are shown in Table 10 for process times of 2 h, 4 h and 6 h.

Table 10: Post Hoc Time Comparisons from Tukey's test at 60 °C.

Time (h)	Time (h)	Average diference	Standard deviation	DF	T	p_{tukey}
2	4	-1.78	0.285	30	-6.27	< 0.001
	6	-3.89	0.298	30	-13.05	< 0.001
4	6	-2.11	0.298	30	-7.07	< 0.001

Obs: DF = degrees of freedom; T = T-value; pTukey = adjusted p-value

Source: elaborated by the authors.

Results from Table 10 indicated that there was significant variance in compressive strength between 2 h and 4 h and also between 4 h and 6 h. These results and the data of Table 6 allowed the conclusion that longer process times resulted in higher strength.

The analysis on the effect of pressure on the accelerated carbonation process at 60 °C was also conducted with a Post Hoc Tukey's test. Results are shown in Table 11 for pressures of 5 bar, 10 bar, 40 bar and 60 bar.

Table 11: Post Hoc Pressure Comparisons from Tukey's test at 60 °C.

Comparison						
Time (h)	Time (h)	Average diference	Standard deviation	DF	T	p_{tukey}
2	4	-1.78	0.285	30	-6.27	< 0.001
	6	-3.89	0.298	30	-13.05	< 0.001
4	6	-2.11	0.298	30	-7.07	< 0.001

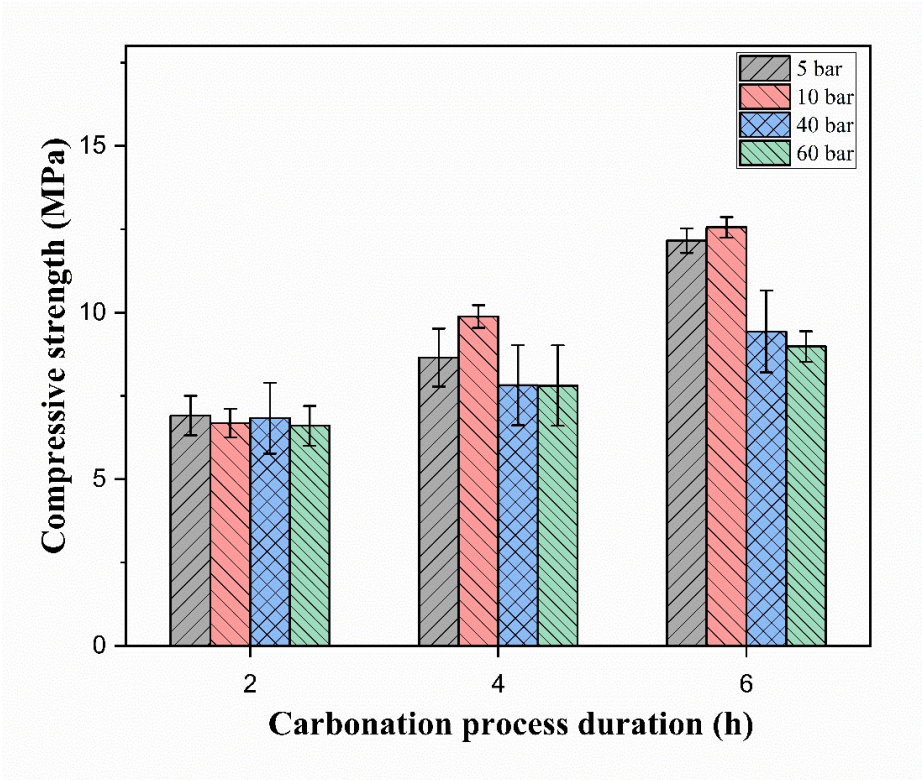
Obs: DF = degrees of freedom; T = T-value; pTukey = adjusted p-value

Source: elaborated by the authors.

Results of Table 11 show that there was no significant variation in compressive strength between 5 bar and 10 bar and also between 40 bar and 60 bar. However, there were significant differences between 5 bar and both 40 bar and 60 bar, as well between 10 bar and both 40 bar and 60 bar. These results and the data of Table 6 confirmed that higher process pressures hampered the development of compressive strength.

Figure 8 presents compressive strength results for a temperature of 60 °C grouped by process time and CO_2 pressure alongside standard deviation bars. Results reflect trends in accordance with the variation of controlled factors evaluated and presented in Tables 9, 10 and 11.

Figure 8: Compressive strength of EAFS mortar subjected to accelerated activation at 60 °C grouped by time and CO_2 pressure.



Source: elaborated by the authors.

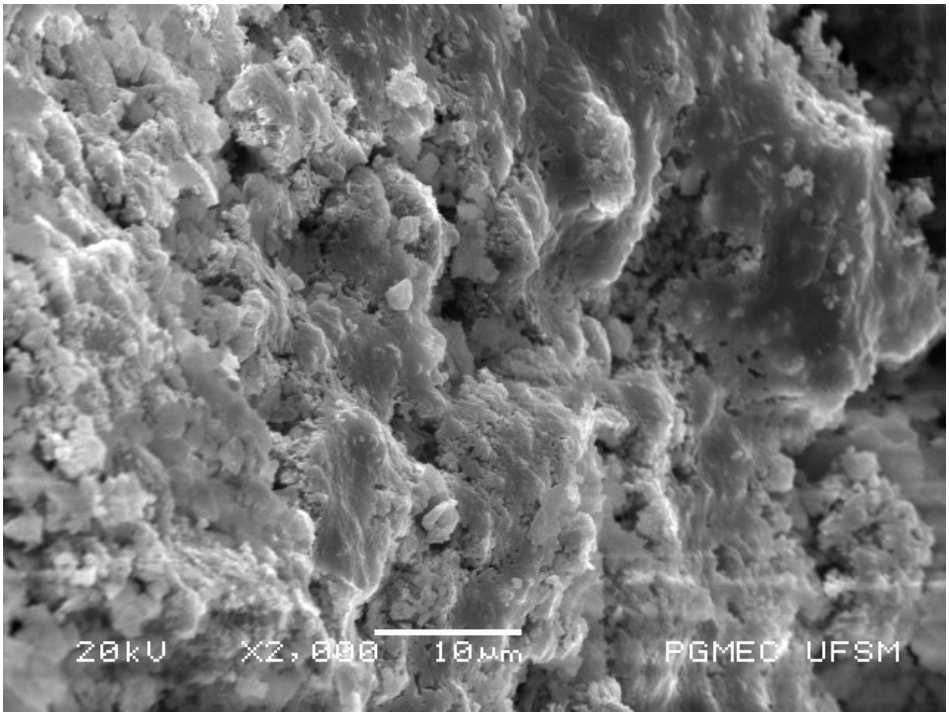
Figure 8 shows that, in general, processes at 60 °C with the lower CO_2 pressures of 5 bar and 10 bar developed higher strength for all times tested (2 h, 4 h and 6 h) when compared to the higher pressures of 40 bar and 60 bar. However, for a process time of 2 h, all applied pressures (5 bar, 10 bar, 40 bar and 60 bar) did not affect strength significantly at this temperature. But when considering process times of 4 h and 6 h, strength increased both with the increases in pressure of 5 bar and 10 bar and longer process time. Similarly, no substantial increases in strength were observed for process times of 4 h and 6 h and higher pressures of 40 bar and 60 bar. These results were in agreement with Table 11 which demonstrated no significant difference in the development of strength between pressures of 40 bar and 60 bar.

Figure 8 demonstrated that longer accelerated carbonation process times were related to increases in compressive strength. Zhong *et al*. (2021) also obtained increased strength in steelmaking slag mortars from a basic oxygen furnace activated with accelerated carbonation process times of 2 h and 6 h. In addition, Li *et al*. (2022) confirmed increased strength in EAF slag blocks with accelerated carbonation process times between 2 h and 6 h. These references were in agreement with the results of Tables 9 and 10 which indicated process time as the most significant factor in the development of compressive strength in the EAFS of this study.

4.6 SEM

The morphology of the fracture surface of mortar specimens subjected to accelerated carbonation under the condition that yielded the highest compressive strength, designated as 60c-5b-6h, was investigated by scanning electron microscopy (SEM) using fragments collected after the axial compressive strength test. Figure 9 presents the SEM micrograph of the specimen corresponding to the 60c-5b-6h condition at a magnification of 2000x.

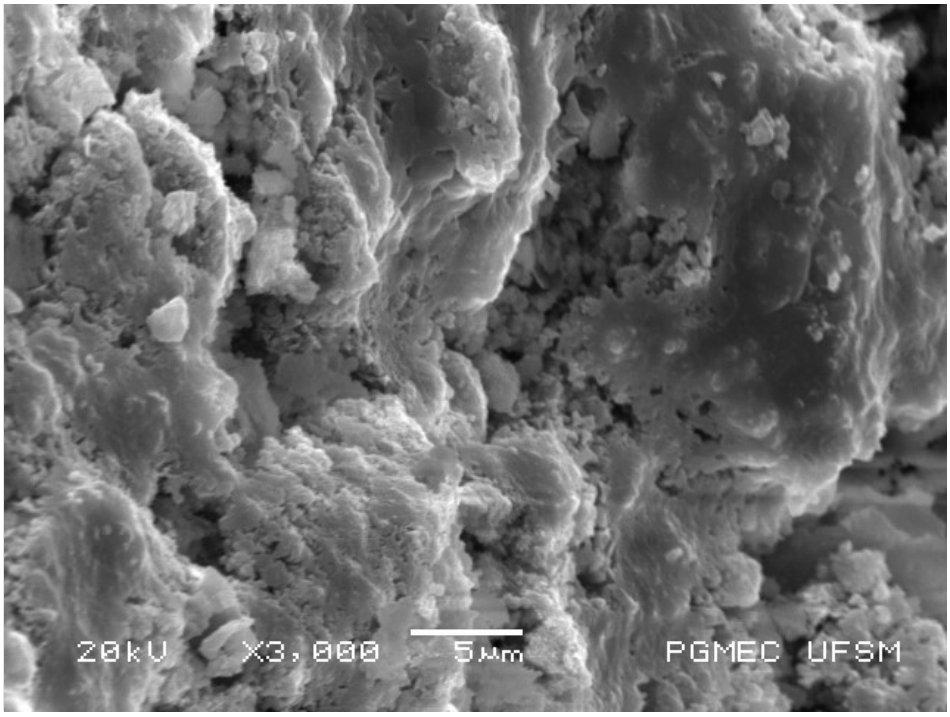
Figure 9: Scanning electron micrograph of the fracture surface of EAF slag-based mortar subjected to accelerated carbonation at 60°C, 5 bar, and 6 h of exposure (2000x).



Source: elaborated by the authors.

As shown in Figure 9, the 60c-5b-6h mortar specimen exhibits a significantly densified microstructure, characterized by an irregular morphology within the binder matrix. Furthermore, no unreacted slag particles were identified within the matrix, and the morphology of the binder phase differs significantly from that observed in the initial condition presented in Figure 1. These microstructural changes suggest the formation of reaction products resulting from the interaction between the activated slag and CO_2 under pressurized carbonation conditions. It is also hypothesized that the morphology observed in Figure 9 was influenced by the hydration of calcium silicate-based compounds, promoting the formation of C-S-H phases, as discussed by Lodeiro *et al*. (2009). Figure 10 presents a micrograph acquired at a magnification of 3000× focusing on the activated slag matrix region highlighted in Figure 9.

Figure 10: Scanning electron micrograph of the fracture surface of EAF slag-based mortar subjected to accelerated carbonation at 60°C, 5 bar, and 6 h of exposure (3000×).



Source: elaborated by the authors.

The fracture surface of the 60c-5b-6h specimen, illustrated in Figures 9 and 10, reveals the presence of clusters of polygonal structures with approximate dimensions of 5-10 µm, which were likely formed as a result of the EAF slag activation process. These features appear to be distributed throughout the matrix and contribute to the compact morphology observed in the specimen.

The carbonation duration likely played a decisive role in the densification of the evaluated matrices. Vargas (2023), when investigating accelerated carbonation in mortars produced with ground granulated blast furnace slag for carbonation periods of 2 and 6 h, also observed that longer exposure times resulted in more densified regions, whereas shorter carbonation periods favored the development of more porous transition zones. Similarly, Zhong *et al*. (2021), in their evaluation of pastes produced with basic oxygen furnace steel slag, reported that increasing carbonation time promoted greater matrix densification, which was associated with the development of calcite crystals.

5 CONCLUSIONS

This study evaluated the accelerated carbonation of mortar produced with electric arc furnace slag

(EAFS) from steel making. Processes were conducted with 4 different CO_2 pressures (5 bar, 10 bar, 40 bar and 60 bar), 3 different temperatures (40 °C, 60 °C and 80 °C) and 3 different process times (2 h, 4 h and 6 h). The following conclusions were drawn:

•Statistical analysis indicated process time was the only significant factor in the development of compressive strength for temperatures of 40 °C and 80 °C;

•For a temperature of 60 °C, both process time and CO_2 pressure were significant factors. Therefore, this temperature was deemed as ideal for the accelerated carbonation of the EAFS of this study;

•Statistical analysis indicated that higher increases in strength were achieved with the lower CO_2 pressures of 5 bar and 10 bar. Strength was also found to decrease as pressure further increased to 40 bar and 60 bar;

•Process time was identified as a significant factor in the increase of compressive strength of all samples. Strength continuously increased up to the longest time of 6 h evaluated in this study;

•The compressive strength of the ideal process took under consideration the lower energy cost of the lowest pressure for a combination of 60 °C, 5 bar and 6 h. The resulting strength of 12.16 MPa was compared to the highest strength of control mortars not subjected to accelerated carbonation (0.97 MPa) and produced an increase of approximately 1,154 %;

•SEM analysis of the 60c-5b-6h specimen revealed a densified microstructure, characterized by a homogeneous matrix, reduced porosity, and good adhesion between the activated binder and the sand grains. The observed morphology suggests a high degree of EAF slag reaction and the formation of reaction products capable of refining the microstructure, thereby directly contributing to the increase in compressive strength.

Activation from accelerated carbonation was demonstrated to be a technique with multiple benefits: it converts steel making waste into a valuable agglomerate with notable mechanical properties while also sequestering CO_2 in its matrix. Moreover, the process also consumes CO_2 making it a viable technique for the development of low-carbon construction materials, and promotes a circular economy cycle by integrating both metallurgy and construction sectors.

ACKNOWLEDGEMENTS

The authors would like to express their sincere gratitude to CNPq (Conselho Nacional de Desenvolvimento Científico e Tecnológico) and CAPES (Coordenação de Aperfeiçoamento de Pessoal de Nível Superior) for the financial support that made this research possible. The authors also gratefully acknowledge the Laboratório de Microscopia (MEV) of the Universidade Federal de Santa Maria (UFSM) for

providing access to the scanning electron microscopy facilities and laboratory infrastructure used in this study. Finally, the authors thank Mr. Vilson Machado Tombezi, laboratory technician at UFSM, for his invaluable technical assistance, expertise, and continuous support throughout the experimental program.

REFERENCES

AKBARI, M.; DANESHMAND, S.; HEYDARI VINI, M.; AZIMY, H. Effect of roasting process on the V (anti-tumor agent) recovery from the slag of the electric arc furnace (EAF). **Heliyon**, v. 10, n. 11, p. e31986, 2024.

ANDRADE, H. D.; CARVALHO, J. M. F.; COSTA, L. C. B.; ELÓI, F. P. F.; SILVA, K. D. C.; PEIXOTO, R. A. F. Mechanical Performance and Resistance to Carbonation of Steel Slag Reinforced Concrete. **Construction and Building Materials**, v. 298, 2021, 123910. Available at: https://doi.org/10.1016/j.conbuildmat.2021.123910.

ANDREW, R. M.: Global CO2 emissions from cement production, 1928-2018, **Earth Syst. Sci. Data**, 11, 1675-1710, https://doi.org/10.5194/essd-11-1675-2019, 2019.

ASSOCIAÇÃO BRASILEIRA DE NORMAS TÉCNICAS (ABNT). **NBR 7215: Portland Cement - Determination of Compressive Strength of Cylindrical Specimens**. Rio de Janeiro: ABNT, 2019.

BAUER, L. **Estimation of the Weighted Spearman Correlation Coefficient**. Master's Dissertation in Epidemiology. Federal University of Rio Grande do Sul (UFRGS), Porto Alegre, 2007. Available at: https://lume.ufrgs.br/handle/10183/11499.

BIAVA, G., DEPERO, L.E., BONTEMPI, E., 2024. Accelerated carbonation of steel slag and their valorisation in cement products: a review. **Spanish Journal of Soil Science**. 14, 12908. https://doi.org/10.3389/sjss.2024.12908.

BUSTAMANTE, M.; MUÑOZ, J.; MUÑOZ, P.; LETELIER, V. Study of mortars with total replacement of electric arc furnace slag aggregates carbonated by aqueous processes. **Construction and Building Materials**, v. 463, 2025. Available at: http://dx.doi.org/10.1016/j.conbuildmat.2025.143890.

CAO, Y.; WANG, Y.; ZHANG, Z.; WANG, H. Recycled sand from sandstone waste: A new source of high-quality fine aggregate. Resources, **Conservation and Recycling**, v. 179, 2022. Available at: http://dx.doi.org/10.1016/j.resconrec.2021.106116.

CARVALHO, V. R.; BAÊTA, B. E. L.; COSTA, L. C. B.; PEIXOTO, R. A. F. Dual admixtures for cement-based composites comprising steel slag powder and residual lignin-based liquor. **Journal of Cleaner Production**, 2024. Available at: http://dx.doi.org/10.1016/j.jclepro.2024.143639.

CARVALHO, V. R.; COSTA, L. C. B.; ELÓI, F. P. F.; BEZERRA, A. C. S.; CARVALHO, J. M. F.; PEIXOTO, R. A. F. Performance of Low-Energy Steel Slag Powders as Supplementary Cementitious Materials. **Construction and Building Materials**, v. 392, 2023, 131888. Available at: https://doi.org/10.1016/j.conbuildmat.2023.131888.

CHEN, Z.; CUI, J.; LIU, Y.; JING, X.; HE, B.; CANG, D.; ZHANG, L. Enhancing Temperature Resistance of Calcium Aluminate Cement through Carbonated Steel Slag. **Journal of Building Engineering**, v. 102, 2025, 111956. Available at: https://doi.org/10.1016/j.jobe.2025.111956.

CHRISTMAS, K. M.; BASSINGTHWAIGHTE, J. B. Equations for O_2 and CO_2 Solubilities in Saline and Plasma: Combining Temperature and Density Dependences. **Journal of Applied Physiology**, v. 122, n. 5, p. 1313-1320, 2017. Available at: http://www.jappl.org1313.

COSME, J.; FERNANDES, G. Steel slag aggregate as a sustainable alternative to railway ballast: Field and laboratory evaluation. **Transportation Geotechnics**, 2025. Available at: http://dx.doi.org/10.1016/j.trgeo.2025.101705.

CRISTINO, L.S., 2024. **Thermal properties of electrical arc furnace slag-based materials obtained by accelerated carbonation**. Thesis. Available at: http://hdl.handle.net/10400.6/14528.

DANCEY, C.; REIDY, J. **Statistics without Mathematics for Psychology**: Using SPSS for Windows. Porto Alegre: Penso, 2019.

DENG, P.; ZHENG, Z. Mechanical properties of one-part geopolymer masonry mortar using alkali-fused lead-zinc tailings. **Construction and Building Materials**, v. 362, 2023. Available at: http://dx.doi.org/10.1016/j.conbuildmat.2023.130522.

DERENSY, M.; TÖNNESEN, T. From metallurgical waste to sustainable refractory binder: Hydraulic performance of vanadium-bearing slags. **Ceramics International**, 2026. Available at: http://dx.doi.org/10.1016/j.ceramint.2026.03.464.

DEUS, A. C. F.; BÜLL, L. T.; GUPPY, C. N.; SANTOS, S. M. C.; MOREIRA, L. L. Q. Effects of Lime and Steel Slag Application on Soil Fertility and Soybean Yield under a No-Till System. **Soil and Tillage Research**, v. 196, p. 104422, 2020. Available at: http://dx.doi.org/10.1016/j.still.2019.104422.

DIGIOVANNI, C., ECHTERHOF, T., 2024. Progress toward biocarbon utilization in electric arc furnace steelmaking: current status and future prospects. **Journal of Sustainable Metallurgy**. 10, 2047-2067. https://doi.org/10.1007/s40831-024-00940-0.

GHOULEH, Z., GUTHRIE, R.I.L., SHAO, Y., 2015. High-strength KOBM steel slag binder activated by carbonation. **Construction and Building Materials**. 99, 175-183. https://doi.org/10.1016/j.conbuildmat.2015.09.006.

GUIMARÃES, A. C. R.; COSTA, K. Á.; REIS, M. M.; SANTANA, C. S. A.; CASTRO, C. D. Study of Controlled Leaching Process of Steel Slag in Soxhlet Extractor Aiming Employment in Pavements. **Transportation Geotechnics**, v. 27, 2021, 100485. Available at: https://doi.org/10.1016/j.trgeo.2020.100485.

GUO, Y.; SHEN, L.; ZHANG, H.; CHEN, Z.; WANG, Y.; ZHANG, X. A Review of Low-Carbon Technologies and Projects for the Global Cement Industry. **Journal of Environmental Sciences**, v. 136, p. 682-697, 2024. Available at: http://dx.doi.org/10.1016/j.jes.2023.01.021.

HEBEDA, O.; GUIMARÃES, B. S.; CRETTON-SOUZA, G.; LA ROVERE, E. L.; PEREIRA, A. O. Pathways for Deep Decarbonization of the Brazilian Iron and Steel Industry. **Journal of Cleaner Production**, v. 401, 2023, 136675. Available at: https://doi.org/10.1016/j.jclepro.2023.136675.

HONG, Z.; HU, C.; LENG, Y.; YIN, T.; YU, R. Exploring the optimal carbonation curing condition for high-performance mortar with different dosages of reactive solid waste powder. **Journal of Building Engineering**, v. 123, p. 115818, 2026. Available at: http://dx.doi.org/10.1016/j.jobe.2026.115818.

HWALLA, J.; EL-HASSAN, H.; ASSAAD, J. J.; EL-MAADDAWY, T.; BAWAB, J. Effect of Type of Sand on the Flowability and Compressive Strength of Slag-Fly Ash Blended Geopolymer Mortar. **Proceedings of the 8th International Conference on Civil, Structural and Transportation Engineering (ICCSTE'23)**, Canada, 2023. Available at: http://dx.doi.org/10.11159/iccste23.115.

International Energy Agency (IEA), 2021. **Net zero by 2050 - a roadmap for the global energy sector**. OECD Publishing, Paris. https://doi.org/10.1787/c8328405-en.

IPCC, 2023: Climate Change 2023: Synthesis Report. **Contribution of Working Groups I, II and III to the Sixth Assessment Report of the Intergovernmental Panel on Climate Change.** Core Writing Team, H. Lee and J. Romero. IPCC, Geneva, Switzerland,

JAMOVI. jamovi. Version 2.3.21 [Computer Software], 2024. Available at: https://www.jamovi.org.

KO, M.S., CHEN, Y.L., JIANG, J.H., 2015. Accelerated carbonation of basic oxygen furnace slag and the effects on its mechanical properties. **Construction and Building Materials**. 98, 286-293. https://doi.org/10.1016/j.conbuildmat.2015.08.051.

LI, J.; WU, S.; HUANG, Y.; LI, Z.; LI, J.; SHI, Y. Carbonation performance and environmental assessment of alkali-activated slag-fly ash-steel slag mortars: Precursor composition effects revealed by quantitative carbonate zoning. **Environmental Research**, v. 288, Part 1, p. 123252, 2026. Available at: http://dx.doi.org/10.1016/j.envres.2025.123252.

LI, L.; ZHONG, X.; LING, T.-C. Effects of accelerated carbonation and high temperatures exposure on the properties of EAFS and BOFS pressed blocks. **Journal of Building Engineering**, v. 45, p. 103504, 2022. Available at: http://dx.doi.org/10.1016/j.jobe.2021.103504.

LIU, P.; ZHONG, J.; ZHANG, M.; MO, L.; DENG, M. Effect of CO_2 treatment on the microstructure and properties of steel slag supplementary cementitious materials. **Construction and Building Materials**, v. 309, p. 125171, 2021. Available at: http://dx.doi.org/10.1016/j.conbuildmat.2021.125171.

LODEIRO, I. G; MACPHEE, D. E.; PALOMO, A.; FERNÁNDEZ-JIMÉNEZ Effect of Alkalis on Fresh C-S-H Gels. FTIR Analysis. **Cement and Concrete Research**, v. 39, n. 3, p. 147-153, 2009. Available at: http://dx.doi.org/10.1016/j.cemconres.2009.01.003.

LOODTS, V.; RONGY, L.; DE WIT, A. Impact of Pressure, Salt Concentration, and Temperature on the Convective Dissolution of Carbon Dioxide in Aqueous Solutions. **Chaos**, v. 24, n. 4, p. 043120, 2014. Available at: http://dx.doi.org/10.1063/1.4896974.

LUO, Z., WANG, Y., YANG, G., YE, J., ZHANG, W., LIU, Z., MU, Y., 2021. Effect of curing temperature on carbonation behavior of steel slag compacts. **Construction and Building Materials**. 291, 123369. https://doi.org/10.1016/j.conbuildmat.2021.123369.

MANERA, C.; PERONDI, D.; RESTELATTO, D.; GODINHO, M.; VILELA, A. C. F. Study of Chlorine Removal from Shredder Residue: Thermal Dechlorination and Water Leaching. **Sustainable Chemistry for the Environment**, v. 6, 2024, 100091. Available at: https://doi.org/10.1016/j.scenv.2024.100091.

MO, L.; HAO, Y.; LIU, Y.; WANG, F.; DENG, M. Preparation of Calcium Carbonate Binders via CO_2 Activation of Magnesium Slag. **Cement and Concrete Research**, v. 121, p. 81-90, 2019. Available at: http://dx.doi.org/10.1016/j.cemconres.2019.04.005.

NGUYEN, T. N.; PHUNG, Q. T.; FREDERICKX, L.; JACQUES, D.; DAUZERES, A.; ELSEN, J.; PONTIKES, Y. Microstructural Evolution and Its Impact on the Mechanical Strength of Typical Alkali-Activated Slag Subjected to Accelerated Carbonation. **Developments in the Built Environment**, v. 19, 2024, 100519. Available at: https://doi.org/10.1016/j.dibe.2024.100519.

PAN, S.-Y.; CHEN, Y.-H.; FAN, L.-S.; KIM, H.; GAO, X.; LING, T.-C.; CHIANG, P.-C.; PEI, S.-L.; GU, G. CO_2 Mineralization and Utilization by Alkaline Solid Wastes for Potential Carbon Reduction. **Nature Sustainability**, v. 3, p. 399-405, 2020. Available at: http://dx.doi.org/10.1038/s41893-020-0486-9.

PAN, S.-Y.; LIU, H.-L.; CHANG, E.-E.; KIM, H.; CHEN, Y.-H.; CHIANG, P.-C. Multiple Model Approach to Evaluation of Accelerated Carbonation for Steelmaking Slag in a Slurry Reactor. **Chemosphere**, v. 154, p. 63-71, 2016. Available at: http://dx.doi.org/10.1016/j.chemosphere.2016.03.093.

PCZIECZEK, A., EFFTING, C., GOMES, I.R., SCHACKOW, A., HENNING, E., 2019. Statistical analysis of mechanical properties of mortars with fly ash and waste tire rubber. **Revista IBRACON de Estruturas e Materiais**. 12(4), 790-811. https://doi.org/10.1590/s1983-41952019000400004.

RAMEZANI, A.; MOODI, F.; MIRABRISHAMI, M.; ZOLFAGHARNASAB, A.; BAHMAN-ZADEH, F. Experimental and Thermodynamic Investigating of Carbonation Behavior in Alkali-Activated Slag-Calcined Clay Materials with Different Binder Constituent. **Construction and Building Materials**, v. 446, 2024, 137987. Available at: https://doi.org/10.1016/j.conbuildmat.2024.137987.

RENFORTH, P.; CAMPBELL, J.; FOTEINIS, S.; COSGUN, E.; YOUNG, J.; STRUNGE, T.; RILEY, A. L.; MAYES, W. M.; VAN DER SPEK, M. W. Carbon Dioxide Removal Could Result in the Use of Lower-Grade Iron Ore in a Decarbonized Net-Negative Emission Steel Industry. **Journal of Cleaner Production**, v. 468, p. 142987, 2024. Available at: http://dx.doi.org/10.1016/j.jclepro.2024.142987.

RODRIGUES, K. H. P.; SILVA, T. O.; PITANGA, H. N.; PEDROTI, L. G.; RODRIGUES, M. H. R. Experimental Study of Mixtures Soil-Industrial Waste Using Simplex Design for Application in Paving. **Journal of Building Engineering**, v. 78, p. 107761, 2023. Available at: http://dx.doi.org/10.1016/j.jobe.2023.107761.

SRIVASTAVA, S.; SNELLINGS, R.; COOL, P. Clinker-Free Carbonate-Bonded (CFCB) Products Prepared by Accelerated Carbonation of Steel Furnace Slags: A Parametric Overview of the Process Development. **Construction and Building Materials**, v. 303, p. 124556, 2021. Available at: http://dx.doi.org/10.1016/j.conbuildmat.2021.124556.

SU, Z.; YUE, Z.; MARSH, A. T. M.; DI MICHIEL, M.; BURNETT, T. L.; PROVIS, J. L.; PAUL, P. P.; BERNAL, S. A.; WITHERS, P. J. 4D Quantification of C-(A)-S-H and Mg-Al LDH Phase Alterations and Microstructural Evolution during Accelerated Carbonation of Alkali-Activated Slag Pastes. **Cement and Concrete Research**, v. 198, p. 108009, 2025. Available at: http://dx.doi.org/10.1016/j.cemconres.2025.108009.

SUKMAK, P.; SUKMAK, G.; DE SILVA, P.; HORPIBULSUK, S.; KASSAWAT, S.; SUDDEEPONG, A. The potential of industrial waste: Electric arc furnace slag (EAF) as recycled road construction materials. **Construction and Building Materials**, v. 368, p. 130393, 2023. Available at: https://www.sciencedirect.com/science/article/pii/S0950061823001046.

SUN, X.; LIU, J.; ZHAO, Y.; ZHAO, J.; LI, Z.; SUN, Y.; QIU, J.; ZHENG, P. Mechanical Activation of Steel Slag to Prepare Supplementary Cementitious Materials: A Comparative Research Based on the Particle Size Distribution, Hydration, Toxicity Assessment and Carbon Dioxide Emission. **Journal of Building Engineering**, v. 60, p. 105200, 2022. Available at: http://dx.doi.org/10.1016/j.jobe.2022.105200.

UNITED NATIONS ENVIRONMENT PROGRAMME (UNEP). **Global Status Report for Buildings and Construction 2024/2025: Not Just Another Brick in the Wall - The Solutions Exist. Scaling Them Will Build on Progress and Cut Emissions Fast**. Paris: United Nations Environment Programme, 2025. Available at: https://wedocs.unep.org/20.500.11822/47214.

WANG, H.; LAWAL, T.; ACHOUR, S. H.; SHENG, K.; OKUNO, R. Aqueous Nanobubble Dispersion of CO_2 at Pressures Up To 208 bara. **Energy & Fuels**, v. 37, n. 24, 2023. Available at: http://dx.doi.org/10.1021/acs.energyfuels.3c03660.

WANG, K.; LEI, Y.; ZHA, X. Mechanical and carbonation performance of alkali-activated mortars incorporating GGBS and recycled construction spoil. **Buildings**, v. 16, n. 2, 2026. Available at: http://dx.doi.org/10.3390/buildings16020453.

WEIDE, H. **Evaluation of the Macrostructural and Microstructural Properties of Slag-Based Binders Activated by Accelerated Carbonation**. Master's Dissertation in Civil Engineering. Federal University of Santa Maria, Santa Maria, 2023. Available at: https://repositorio.ufsm.br/handle/1/33427.

WU, W.; LI, Y.; DU, X.; ZHAO, H.; KONG, J.; WANG, L.; CHEN, M.; QUAN, H. Formulation and Characterization of One-Part Ca-Based Alkali-Activated Slag-Steel Slag Materials. **Construction and Building Materials**, v. 449, p. 138432, 2024. Available at: http://dx.doi.org/10.1016/j.conbuildmat.2024.138432.

XAVIER, L. A.; FETZER, D. E. L.; OLIVEIRA, T. V.; EIRAS, D.; VOLL, F. A. P.; VIEIRA, R. B. Effect of Stainless-Steel Slag Concentration in the Fabrication of Cost-Effective Ceramic Membranes: Seawater Pre-Treatment Application. **Ceramics International**, v. 48, n. 16, p. 23273-23283, 2022. Available at: https://doi.org/10.1016/j.ceramint.2022.04.312.

YI, Y.-R.; LIN, Y.; DU, Y.-C.; BAI, S.-Q.; MA, Z.-L.; CHEN, Y.-G. Accelerated Carbonation of Ladle Furnace Slag and Characterization of Its Mineral Phase. **Construction and Building Materials**, v. 276, p. 122235, 2021. Available at: http://dx.doi.org/10.1016/j.conbuildmat.2020.122235.

YILDIRIM, I. Z.; PREZZI, M. Chemical, Mineralogical, and Morphological Properties of Steel Slag. **Advances in Civil Engineering**, v. 2011, Article ID 463638, 2011. Available at: http://dx.doi.org/10.1155/2011/463638.

ZHANG, T.; WU, J.; CHEN, M.; HONG, Y. Utilization of Carbonation-Treated Steel Slag as Fine Aggregates to Enhance the Mechanical Properties and Microstructural Evolution of Cement Mortar. **Journal of Sustainable Cement-Based Materials**, v. 15, n. 3, p. 866-884, 2026. Available at: http://dx.doi.org/10.1080/21650373.2025.2582162.

ZHAO, S.; LIU, Z.; WANG, F.; HU, S. Elucidating factors on the strength of carbonated compacts: Insights from the carbonation of γ-C_2S, β-C_2S and C_3S. **Cement and Concrete Composites**, v. 156, 2025. Available at: http://dx.doi.org/10.1016/j.cemconcomp.2024.105806.

ZHONG, X.; LI, L.; JIANG, Y.; LING, T.-C. Elucidating the Dominant and Interaction Effects of Temperature, CO_2 Pressure and Carbonation Time in Carbonating Steel Slag Blocks. **Construction and Building Materials**, v. 302, p. 124158, 2021. Available at: http://dx.doi.org/10.1016/j.conbuildmat.2021.124158.

ZHOU, Q.; LI, G.; YUAN, K.; SU, Y.; SHAO, N.; BAI, W.; SHEN, X.; ZHANG, Z. Pore Structure and Strength Evolution in Alkali-Activated Slag Mortars Induced by Accelerated Carbonation. **Metallurgical and Materials Transactions B: Process Metallurgy and Materials Processing Science**, v. 57, p. 1765-1775, 2026. Available at: http://dx.doi.org/10.1007/s11663-026-03955-y.